Electrochimica Acta, 1967, Vol. 12, pp. 1441 to 1455. Pergamon Press Ltd. Printed in Northern Ireland

KINETICS OF THE DISCHARGE OF NITRITE IONS IN THE ELECTROLYSIS OF MOLTEN NITRITES ON GRAPHITE ELECTRODES*

A. J. ARVÍA and A. J. CALANDRA
Instituto Superior de Investigaciones, Facultad de Química y Farmacia,
Universidad Nacional de La Plata, La Plata, Argentina

Abstract—The discharge of nitrite ions in the electrolysis of molten nitrites on graphite electrodes of known porosity has been studied in the temperature range 245–340°C.

Conventional current/voltage curves, and build-up and decay of the working electrode potential, were determined. In the whole range of current density and temperature investigated the anodic process is characterized by a Tafel slope of $2RT/3F$. Decay and Tafel slopes tend to coincide at the highest current densities.

Electrode capacitance measurements at the initial potential suggest a roughness factor of about 50 for graphite electrodes.

The results are interpreted in terms of the following reaction schemes:

$$NO_2^- + C \rightleftharpoons (NO_2)C + e, \quad \text{(Ia)}$$
$$(NO_2)C + NO_2^- \rightarrow (N_2O_4) + C + e, \quad \text{(IIa)}$$
$$(N_2O_4) \rightleftharpoons 2NO_2, \quad \text{(IIIa)}$$

and

$$NO_2^- + C \rightleftharpoons (NO_2)C + e, \quad \text{(Ia)}$$
$$(NO_2)C \rightarrow NO_2^+ + C + e, \quad \text{(IIb)}$$
$$NO_2^+ + NO_2^- \rightleftharpoons (N_2O_4) \rightleftharpoons 2NO_2, \quad \text{(IIIb)}$$

where either reaction (IIa) or (IIb) is the rate-determining step, assuming a low electrode surface coverage by reaction intermediates.

Data from non-steady measurements are rather scattered and this is ascribed to probable diffusion of nitrogen dioxide through the porous electrode material.

Résumé—La décharge d'ions nitrite sur des électrodes de graphite de porosité connue dans l'electrolyse de nitrites fondus a été étudiée à des températures entre 245 et 340°C.

Les courbes courant-tension et l'accroissement et la décroissance de la tension de l'électrode de travail ont été déterminées. Dans la région de densité de courant et de température étudiée, le processus anodique se caractérise par une pente de Tafel égale à $2RT/3F$. Les pentes obtenues des courbes de décroissance et des courbes courant-tension ont une tendance à coincider à des densités de courant élevées.

Les mesures de la capacité de l'électrode à la tension initiale indiquent un facteur de rugosité d'environ 50 pour les électrodes de graphite.

Les résultats s'interprètent avec les mécanismes suivants:

$$NO_2^- + C \rightleftharpoons (NO_2)C + e, \quad \text{(Ia)}$$
$$(NO_2)C + NO_2^- \rightarrow (N_2O_4) + C + e, \quad \text{(IIa)}$$
$$(N_2O_4) \rightleftharpoons 2NO_2, \quad \text{(IIIa)}$$

et

$$NO_2^- + C \rightleftharpoons (NO_2)C + e, \quad \text{(Ia)}$$
$$(NO_2)C \rightarrow NO_2^+ + C + e, \quad \text{(IIb)}$$
$$NO_2^+ + NO_2^- \rightleftharpoons (N_2O_4) \rightleftharpoons 2NO_2, \quad \text{(IIIb)}$$

où la réaction (IIa) ou (IIb) est l'étape déterminante de la vitesse si on suppose qu'il y a une couverture peu importante de l'électrode par les intermédiaires de la réaction.

Les résultats des mesures non-stationnaires sont plutôt dispersés, ce qui s'attribue à une diffusion probable de dioxyde de nitrogène à travers le matériau poreux de l'électrode.

* Manuscript received 2 January 1967.

Zusammenfassung—Die Entladung von Nitritionen an Graphitelektroden bekannter Porosität in der Elektrolyse geschmolzener Nitrite wurde bei Temperaturen von 245 bis 340°C untersucht.

Es wurden die üblichen Strom-Spannungskurven und das Anwachsen und Abnehmen der Spannung an der Arbeitselektrode bestimmt. Im ganzen Bereich der untersuchten Stromdichten und Temperaturen ist der anodische Vorgang durch eine Tafelgerade der Neigung $2RT/3F$ charakterisiert. Die Spannungsabnahme und das Tafelgefälle zeigen eine Tendenz zur Übereinstimmung bei den höchsten Stromdichten.

Die Elektrodenkapazität-Messungen bei der Anfagsspannung zeigen einen Rauhheitsfaktor von ungefähr 50 für Graphitelektroden.

Die Ergebnisse werden mittels der nachstehenden Reaktions-Schemas interpretiert:

$$NO_2^- + C \rightleftharpoons (NO_2)C + e, \quad \text{(Ia)}$$

$$(NO_2)C + NO_2^- \rightarrow (N_2O_4) + C + e, \quad \text{(IIa)}$$

$$(N_2O_4) \rightleftharpoons 2NO_2, \quad \text{(IIIa)}$$

und

$$NO_2^- + C \rightleftharpoons (NO_2)C + e, \quad \text{(Ia)}$$

$$(NO_2)C \rightarrow NO_2^+ + C + e, \quad \text{(IIb)}$$

$$NO_2^+ + NO_2^- \rightleftharpoons (N_2O_4) \rightleftharpoons 2NO_2, \quad \text{(IIIb)}$$

wo (IIa) oder (IIb) der geschwindigkeitsbestimmende Schnitt ist, wenn man eine geringe Flächenbedeckung der Elektrode durch Zwischenprodukte annimt.

Ergebnisse nicht stationärer Messungen weisen eine ziemliche Streuung auf und dies wird einer wahrscheinlichen Diffusion von Stickstoffdioxyd durch das poröse Elektrodenmaterial zugeschrieben.

INTRODUCTION

THE ELECTROLYSIS of sodium nitrite, potassium nitrite and mixtures of both on platinum electrodes, either as pure nitrites or dissolved at high concentration in a molten nitrate solvent, has been recently studied at various temperatures.[1] In the course of this study a nitrite reversible electrode in the molten state has been discovered.[2] The electrochemical behaviour of dilute solutions of nitrite in molten nitrates had been studied earlier polarographically[3] and more recently voltammetrically.[4–6]

The discharge reaction of pure nitrites was interpreted as an activated electrochemical process where the reaction intermediate compound, (NO_2), was postulated as existing on the electrode surface. With the simple assumption that the intermediate compound follows a Langmuir-type adsorption isotherm, the more likely reaction mechanism can be represented by a reaction scheme involving two alternative steps (i) the desorption of an intermediate yielding nitrogen dioxide and (ii) the simultaneous desorption of two intermediate molecules yielding dinitrogen tetroxide in equilibrium with nitrogen dioxide at working temperature. In this mechanism, the state of the electrode surface was assumed unchanged in the course of the reaction, independently of being totally or partially oxidized, as seems to occur for platinum electrodes in those media, according to recent results.[7] With the previous reaction scheme the experimental Tafel slopes, RT/F and $RT/2F$, obtained from steady current/voltage curves, were satisfactorily explained.

The nitrite solutions were also investigated in a large concentration range under definite hydrodynamic conditions with a platinum rotating disk electrode[8] to evaluate the diffusional contributions involved in the discharge of diluted nitrite ions and to determine the effective diffusion coefficient of the ion in the nitrate melt.

The present work attempts to get further knowledge of the discharge of nitrite ions from pure nitrite melts, particularly concerning the participation of reaction intermediates in the electrode process, when the anodic reaction takes place on graphite electrodes. These electrodes showed very interesting behaviour probably because of

the high density of unpaired electrons of the material,[9] which is the cause of specific interactions between the electrode and the reacting species. This behaviour was already studied in the discharge on nitrate ions on graphite electrodes,[10] where the intermediate (NO_3) formed in the primary electrochemical reaction interacted strongly with the electrode surface forming a C–O bond, essentially affecting the course of the electrode process and yielding nitrogen dioxide and carbon dioxide as reaction products instead of nitrogen dioxide and oxygen, as is the case for the reaction occurring on platinum electrodes.

EXPERIMENTAL TECHNIQUE

The electrolysis cell was almost the same as that described in a previous publication.[1] It consisted of three electrodes placed in independent sections. The working electrodes were made from graphite rods ("National" spectroscopic quality, 3-mm diameter). The apparent electrode area varied from 1 to about 6 cm^2. One end of the electrode was connected to a platinum lead, avoiding contact between the joint both with the melt and with the gases saturating the melt. New and aged graphite electrodes were used, the latter being electrodes that after being used for one set of experiments were left during several weeks exposed to air at room temperature.

Two different reference electrodes, connected with a Luggin–Haber capillary tip arrangement, were used. One consisted of a pure silver wire (Ag-1000) dipped into a solution of silver nitrate (10^{-1} M) in molten sodium-nitrate–potassium-nitrate. In this case the interface between the melts was formed at the side of the capillary tip pointing towards the reference electrode. In this region a slight decomposition of the melt with nitrogen dioxide formation was observed, but this drawback was apparently not important enough to affect the electrode potential measurements, when the experiments were carried out in a reasonable time. The second reference electrode was a platinum wire dipped into the nitrite melt, saturated with nitrogen dioxide. Obviously, the initial potential was different for each electrochemical system, but the same overvoltage/current-density relationship was obtained. The experimental set-up involved a pseudo-ohmic resistance of the order of 0·1 Ω.

A platinum cathode was employed, separated from the rest of the cell by means of a sintered glass disk to minimize the possibility that cathodic products could reach the anodic section of the cell.

The cell was designed to maintain the electrolyte under a controlled atmosphere. Purified nitrogen was bubbled through the melt to eliminate air prior to the electrochemical measurements.

Pure sodium nitrite and mixtures of sodium nitrite and potassium nitrite were employed as electrolytes. The purification, dehydration and preparation of the mixtures were performed with the techniques described elsewhere.[11]

Before any experimental information was obtained, the molten salt was kept for 24–48 h at the temperature of the experiment and electrolysed intermittently at different current densities. Experiments were done in the temperature range 245–340°C taking into account the region where the system was liquid; no appreciable decomposition occurred.

Steady current/voltage curves were recorded at current densities ranging from a few $\mu A/cm^2$ to about 100 mA/cm^2. The galvanostatic method was chosen to obtain polarization curves. These curves were recorded by changing the electrolysis current upwards and downwards to detect any hysterisis effect.

Decay and build-up of the working electrode potential were also measured. For the latter galvanostatic conditions were achieved.

Most of the experiments, under steady as well as non-steady conditions, were performed with the melts previously saturated with nitrogen dioxide formed *in situ* by a preliminary electrolysis.

The rest of the electrical circuitry and the experimental set-up were the same as those already described.[12]

The apparent density and porosity of graphite electrodes were also determined. For the latter an Aminco-Winslow Porosimeter was used.

RESULTS

When molten nitrites are electrolysed on graphite electrodes, nitrogen dioxide, in equilibrium with dinitrogen tetroxide, is the product yielded by the anodic reaction.

1. *Electrode porosity*

Data on apparent density and porosity of graphite electrodes are assembled in Table 1. The pore size distribution shows a maximum value of pore diameter at about 15 μ.

TABLE 1. POROSITY DETERMINATION

Specific volume with He at 20°C 0·18 cm³/g
Apparent specific volume (20°C) 0·62 cm³/g
Specific volume with NO_2 (150°C) 0·32 cm³/g
Porosity with He (20°C), 71·2%
Porosity with NO_2 (150°C), 48·5%
Total porosity of sample, 28·1% (Aminco-Winslow)
Porosity due to pores greater than 76·08 μ diameter 0%
Porosity due to pores less than 0·035 μ diameter, 2·72%
The distribution of pores size indicate a maximum value for a pore diameter of about 15 μ.

2. *Current/voltage relationship*

The current/voltage relationship was established after correction for the pseudo-ohmic overvoltage, which was evaluated from the non-steady measurements. This correction is appreciable only for current densities larger than 5 mA/cm². The overvoltage of the working electrode was plotted against log (current density), referred to the apparent electrode area, as shown in Figs. 1–3. The overvoltage, η, is defined as

$$\eta = E_i - E_\infty, \tag{1}$$

where E_i is the electrode potential at current density i and E_∞ is its steady value after interruption of the electrolysis current.

The overvoltage/log (current density) plot fits quite satisfactorily into a Tafel line, except at current densities below 10 μA/cm². The departure observed in this region is reasonable because of the low overvoltage involved.

Data obtained from the Tafel plots are assembled in Table 2. The Tafel slope, $b_T = \partial\eta/\partial \log i_a$, and the theoretical slope closest to the experimental one are included there. The apparent exchange current density, $(i_0)_{app}$, obtained by extrapolating the Tafel lines to $\eta = 0$, are also shown in the Table.

The most reliable and reproducible results were obtained from experiments

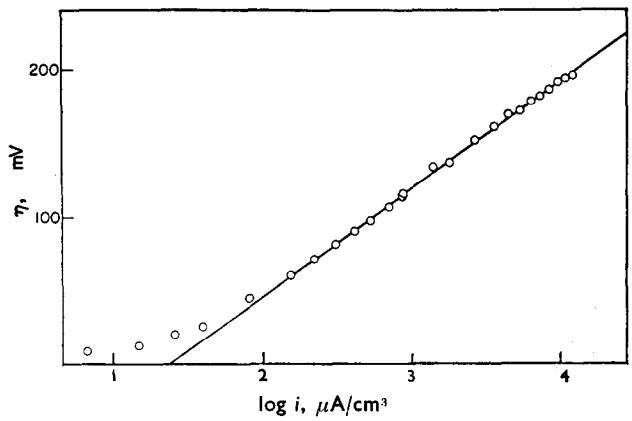

FIG. 1. Tafel plot. $NaNO_2$. 282°C.

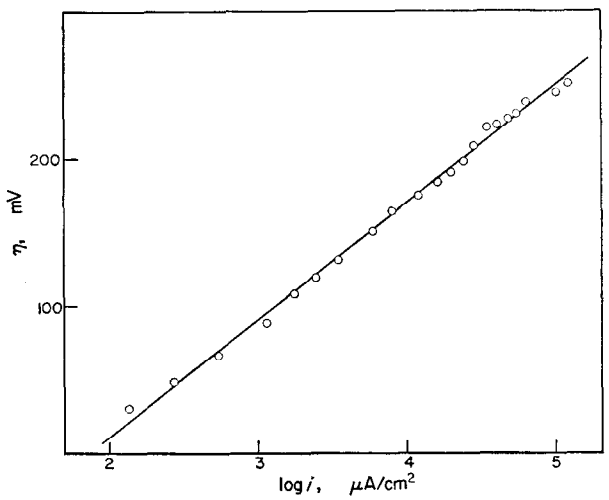

FIG. 2. Tafel plot. KNO_2–$NaNO_2$. 309°C.

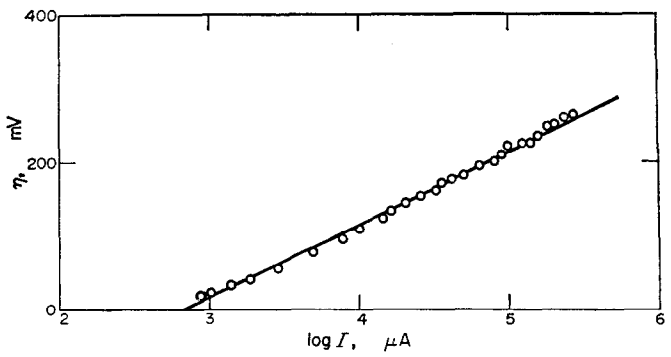

FIG. 3. Tafel plot. Apparent electrode area, 4·88 cm^2. KNO_2–$NaNO_2$. 350°C.

performed with fresh electrodes. When aged electrodes were employed the following effect was observed. The first polarization curve involved the largest overvoltage and after successive experiments, it came closer to the curves obtained with fresh electrodes, as if there was a sort of cleaning effect of the electrode surface during electrolysis. Nevertheless, the reproducibility of results obtained with aged electrodes was not satisfactory enough to allow any straightforward conclusion.

The linear portion of the Tafel line covers from two to three logarithmic decades of current density and has a slope very close to $2{\cdot}3(2RT/3F)$. At the highest current densities employed here, sometimes an overvoltage was observed larger than that expected from the Tafel line. This effect however was later explained after the decay curves were properly analysed, as is described later. It is related to a change of the

TABLE 2

Temp °C	b_T mV	$(i_0 \times 10^4)_{app}$ A/cm²	$(i_0 \times 10^6)_{corr}$ A/cm²	$2{\cdot}3(2RT/3F)$ mV	Electrolyte
249	67 ± 5	3·3	6·6	69·1	$NaNO_2$–KNO_2
283	72	2·3	4·6	73·5	$NaNO_2$
283	73	2·4	4·8	73·5	$NaNO_2$
303	79	1·7	3·4	76·0	$NaNO_2$–KNO_2
303	78	1·2	2·4	76·0	$NaNO_2$–KNO_2
309	80	0·8	1·6	77·0	$NaNO_2$–KNO_2
345	98	1·4	2·8	82·0	$NaNO_2$–KNO_2

rest potential. By taking this change into account, the experimental data can be fitted on the Tafel line that is valid at lower current densities.

The Tafel slope is not affected by temperature. Nevertheless, the apparent exchange current density shows a rather peculiar change with temperature. Above 310°C it increases with temperature while at the lower temperatures, the effect is reversed.

3. *Build-up and decay of electrode potential*

The variation of potential with time was examined either for potential build-up or potential decay, from a few μs up to several min after the electrolysis current was switched on or off, respectively. Build-up and decay curves are shown in Figs. 4–6. From the decay curves the following facts emerge. Initially there is a region where the overvoltage changes rather slowly with log (time), approaching afterwards a region where a linear relationship obtains. The slopes of the best straight lines drawn from this portion, $b_d = -\partial\eta/\partial \log t$, obtained under different experimental conditions, are assembled in Table 3. The values of b_d approach to $2{\cdot}3(2RT/3F)$ for the decay curves at higher current densities. This slope coincides with that already mentioned for the Tafel lines.

It is possible to linearize nearly the whole decay curves by plotting the overvoltage against log $(t + t')$, as shown in Figs. 7 and 8, where t' comprises an experimental pseudocapacitance, C_η, related to the electrode reaction at the interruption potential.[13] Values of t' were obtained by fitting the best straight line. Values of C_η were not evaluated from t' as formerly done[10] because of their non-reproducibility in the present case, but from the initial slope of the decay curves; they are included in Table 4. At constant temperature those figures show a trend towards a slight increase with current density and at constant potential they are fairly independent with temperature.

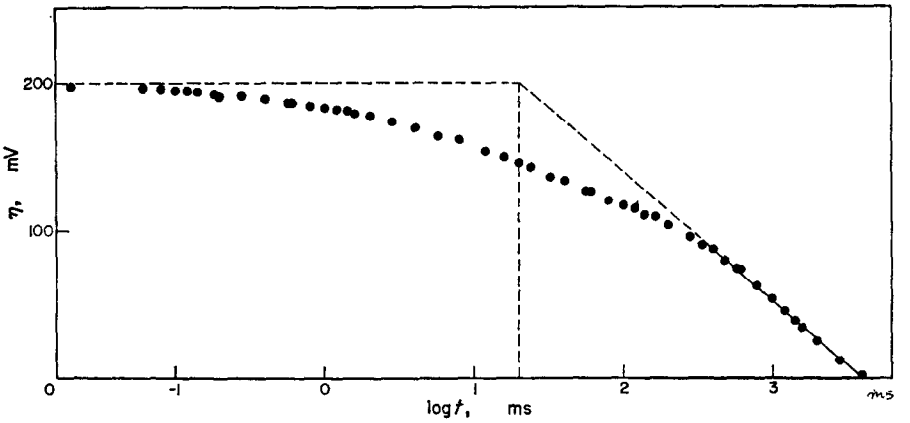

FIG. 4. Semilog plot of decay curve.
KNO_2–$NaNO_2$. 302°C.
i_1, 30·6 mA/cm².

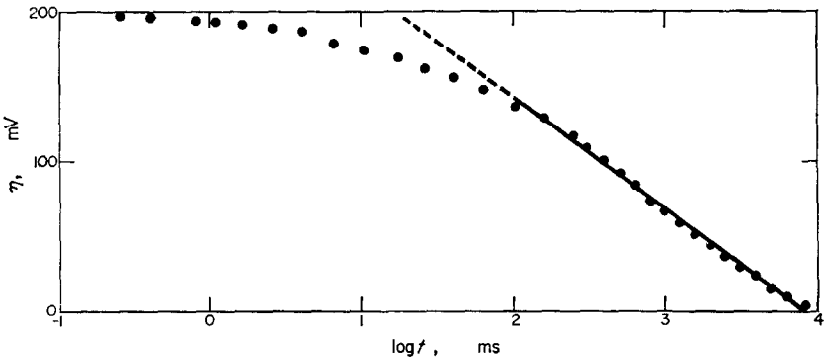

FIG. 5. Semilog plot of decay curves.
KNO_2–$NaNO_2$. 303°C.
i_1, 16 mA/cm².

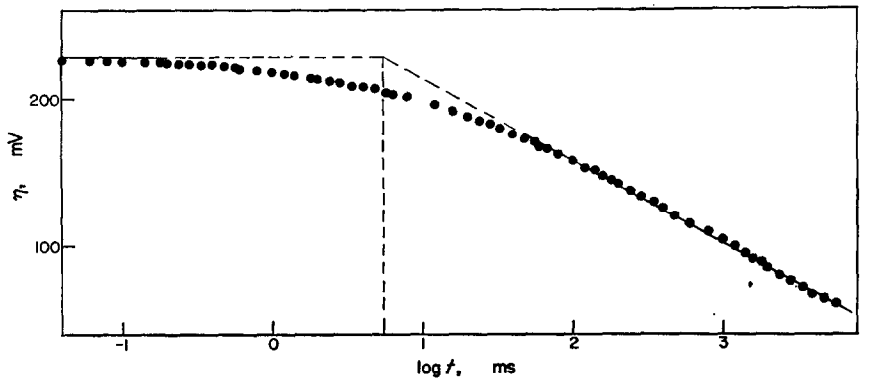

FIG. 6. Semilog plot of decay curves.
KNO_2–$NaNO_2$. 309°C.
i_1, 34·6 mA/cm².

Table 3

Temp. °C	i mA/cm²	b_d mV
253	23·5	50 ± 5
	35·3	52
289	19·2	50
	36·3	52
	82·2	55
297	9·7	76
	16·0	76
	30·7	86
	38·3	76
	20·6	82
308	7·6	57
	57·1	90
337	7·0	60
	17·0	72
	34·0	75
	48·0	78
	70·0	80
350	20·3	70
	53·8	80

Table 4. Electrode differential capacitances

Temp. °C	$(C_{\eta=0})_{app}$ μF/cm²	$(C_{\eta=0})_{corr}$ μF/cm²
	From build-up curves	
282	1500 ± 100	30
	1900	38
	1700	34
308	1400	28
	1500	30
	1500	30

Temp. °C	η mV	$(C_\eta)_{app}$ μF/cm²	$(C_\eta)_{corr}$ μF/cm²
		From decay curves	
274	85	1620 ± 100	32·5
	112	1820	36·5
	123	2260	45·0
350	226	1700	34·0
	270	2000	40·0

The decay curves also show an effect which should be related to a physicochemical change of the electrode surface. The rest potential obtained from decay curves, particularly for the first experiments, increases as the initial current density increases, so that there is a shift of the linear portion of the decay curves in the semilogarithmic plot. This circumstance also produces a shift in the value of t'. However, if the overvoltage is now defined with reference to the particular rest potential, the coincidence of decay curves is again observed. Moreover, if data from the current/voltage curves which deviated from the Tafel line having a slope $2{\cdot}3(2RT/3F)$ are referred to the rest potential obtained from those decay curves, they now fit the just-mentioned Tafel line. It can thus be concluded that the Tafel slope $2RT/3F$ is probably valid for the whole range of current density investigated.

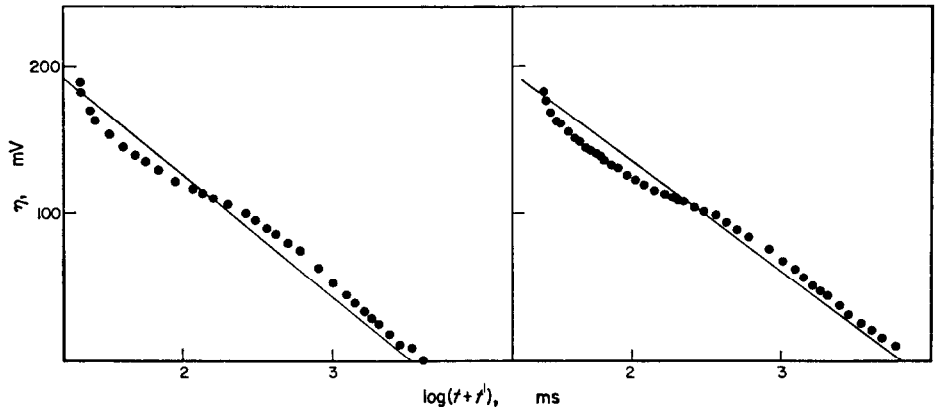

FIG. 7. Plot of decay curve according to equation (14); $t' = 19{\cdot}9$ and $25{\cdot}1$ ms
KNO_2–$NaNO_2$. 303°C.
i_1, 30·7 mA/cm².

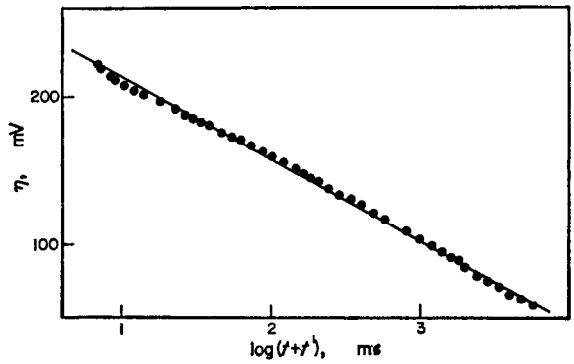

FIG. 8. Plot of decay curves according to equation (14); $t' = 5{\cdot}5$ ms.
KNO_2–$NaNO_2$. 303°C.
i_1, 16·0 mA/cm².

The build-up of potential at constant current occurs much faster than the potential decay. Initially the overvoltage increases linearly with time. From the slope of this linear portion the value of the differential electrode capacitance, $C_{\eta=0}$, at the initial potential was calculated. These values, assembled in Table 4, are practically independent temperature. They should be related to the differential capacitance of the Helmholtz double layer.

4. *The reference potential*

While the working electrode was repeatedly used at different current intensities, a steady rest potential was measured after a certain time starting from the current interruption. This potential lasts as long as the composition of the system is not altered. Values of the emf of the residual cells comprising the working electrode and the reference electrode are shown in Table 5. They are about 12–20 mV lower than those determined for platinum electrodes, but they decrease similarly with temperature. The reproducibility of the rest potential and its dependence on current intensity of the

previous electrolysis were the criteria applied to assume equivalent states of the electrode surface.

DISCUSSION

The facts that the electrode potential after current interruption approaches the values earlier found for platinum electrodes and that no appreciable consumption of the graphite electrodes is observed, indicate that the main anodic reaction is similar to that occurring on platinum anodes and corresponds to the discharge of nitrite ions yielding as final product nitrogen dioxide (in equilibrium with dinitrogen tetroxide),

$$NO_2^- (l) = NO_2(g) + e\,. \qquad (I)$$

Consequently, if the observed effects are mainly assigned to reaction (I), the formation of a nitrite reversible electrode should also take place on the graphite electrodes,

TABLE 5. Emf VALUES OF THE RESIDUAL CELLS COMPRISING A SILVER/SILVER-NITRATE (*ca* 10^{-1} M) ELECTRODE AND A PLATINUM OR GRAPHITE ELECTRODE

Temp °C	E_∞ (graphite) mV	E_∞ (platinum) mV
260 ± 0·5	283 ± 5	330 ± 3
283	215	228
283	210	223
303	108	123
303	106	126

although a small specific effect of the electrode material is noticeable in the shift of the rest potential as compared to the values of the platinum electrodes.

The effect of the nature of the electrode surface on the kinetics of the reaction is however quite evident when the results of the platinum electrodes are compared, under the same experimental conditions, including cell design. This is certainly what is expected for an activated electrochemical process.

In the whole range of current density and temperature investigated there is a satisfactory Tafel relationship, the slope of which is $2RT/3F$. This is one of the most interesting differences between the anodic discharge of nitrite ions on graphite and that on platinum electrodes, where two Tafel slopes are found, RT/F at low current densities and $RT/2F$ at the higher, the transition occurring within a potential region that depends on temperature.[1,2]

On the basis of the Tafel slope and decay slope, the probable mechanism of the anodic reaction may be postulated, although it should be stressed that data obtained from the decay curves are in the present case rather more scattered than those observed in reactions with molten salts previously investigated. However, as decay curves obtained at higher current densities were plotted semilogarithmically, the trend of the decay slope appeared to approach the same value already found from current/voltage curves.

To elaborate a coherent explanation of results it is necessary to take into account two more facts, (i) the apparent exchange current densities, obtained from extrapolation to $\eta = 0$, are approximately 50 times greater than those obtained in the electrolysis of molten nitrites on platinum. (ii) a factor of the same order appears when the

value of the experimental electrode capacitances evaluated at the initial potential are compared with those formerly determined on platinum electrodes. Both facts indicate that the actual graphite electrode area is at least 50 times greater than the apparent area. This figure then may be considered as a sort of roughness factor since the melt in this case wets the electrode surface satisfactorily. It is reasonable, therefore, to refer both the exchange current density as well as the experimental differential capacitances to the actual area. Corrected values are assembled in Tables 2 and 4. The figures are within the correct order of magnitude as far as the anodic reaction is concerned. Also, the value for the roughness of a graphite electrode is in agreement with the values determined for the same kind of electrode in other melts that are known to wet graphite.[14]

When graphite electrodes are used there is another difficulty in interpreting the results, due to the oxidation of the electrode surface, particularly when the latter is in contact with highly oxidizing substances such as nitrogen dioxide. Consequently, the possibility exists that the surface itself induces a further complication if it changes either in the course of the reaction or with the electrode potential. This difficulty is appreciably greater in the non-steady measurements, principally in the decay and build-up curves, and causes a quite important dispersion of results. From the above analysis it is difficult to draw a definite conclusion about any dependence of the experimental electrode capacitance on the electrode potential, although it is possible that the measured quantity might comprise a pseudocapacitance contribution due perhaps to the presence of reaction intermediates.

Looking back to some of the results obtained in the electrolysis of molten nitrites on platinum electrodes,[1,2] it seems now reasonable to assume that the electrode reaction on graphite starts with the discharge of a nitrite ion on the electrode surface. In a simple treatment of the reaction, any particular interference due to the amount of surface oxidation may be either neglected or assumed constant when steady current/voltage curves are measured. If the product yielded by the primary reaction, however, is an (NO_2) radical, some type of interaction may reasonably be expected between that species and the electrode, due to their respective electronic structures. The reaction may further discharge a second nitrite ion on the site where the first intermediate is located, thus yielding a molecule of dinitrogen tetroxide on the electrode in equilibrium with nitrogen dioxide. The reaction scheme can therefore be written as follows:

$$NO_2^- + C \rightleftharpoons (NO_2)C + e, \qquad \text{(Ia)}$$

$$(NO_2)C + NO_2^- \rightarrow (N_2O_4) + C + e, \qquad \text{(IIa)}$$

$$(N_2O_4) \rightleftharpoons 2NO_2. \qquad \text{(IIIa)}$$

The above consecutive reaction scheme involves some interaction of the nitrogen oxides with graphite, which actually occurs, as has been recently shown experimentally.[15]

Reaction (Ia) as the rate-determining step should in principle be discarded, since the experimental Tafel slope is much lower than the theoretical slope $2RT/F$, which is deduced from the kinetic analysis, assuming limiting Langmuir adsorption conditions for the intemediates.

Let us assume that reaction (IIa) is the rate-determining step. The anodic rate equation in terms of current density, i_a, is

$$i_a = 2Fk_{II}a_i a_{NO_2^-} \exp\left[\alpha_{II}\eta F/RT\right], \qquad (2)$$

where k_{II} is the specific rate constant of reaction (IIa), a_i and $a_{NO_2^-}$ are respectively the surface activity of the intermediate and the nitrite ion activity on the electrode surface, η is the electrode overvoltage measured against the reversible nitrite electrode to keep the symmetry of the electrochemical system, and α_{II} is the transfer coefficient assisting reaction (IIa) in the anodic direction. It is assumed that the surface activity of the intermediate is proportional to the degree of surface coverage, X_0: $a_i = k'X_0$. In this circumstance, from the quasi-equilibrium represented by reaction (Ia) we have

$$k_I a_{NO_2^-}(1 - X_0)\exp[\alpha_I \eta F/RT] = k_{-I}X_0 \exp[-(1 - \alpha_I)\eta F/RT]. \quad (3)$$

If it is also assumed that the degree of coverage is low, as is reasonably concluded later, and the transfer coefficient of reaction (Ia), α_I, is taken as 0·5, the following limiting equation is obtained:

$$X_0 = \frac{k_I}{k_{-I}} a_{NO_2^-} \exp[\eta F/RT]. \quad (4)$$

Considering (3) and (4), taking into account that for these pure nitrite melts, $a_{NO_2^-} \approx 1$, and defining the equilibrium constant $K_I = k_I/k_{-I}$, we have

$$i_a = 2FK_I k_{II}' \exp[(1 + \alpha_2)\eta F/RT]. \quad (5)$$

As reaction (IIa) is also a one-electron-transfer process, for a symmetrical reaction co-ordinate, $\alpha_{II} = 0{\cdot}50$, and:

$$1 + \alpha_{II} = \tfrac{3}{2}. \quad (6)$$

Hence

$$i_a = 2FK_I k_{II}' \exp[3\eta F/2RT]. \quad (7)$$

This rate equation involves a Tafel slope for the steady state equal to $2RT/3F$ as experimentally observed.

An alternative explanation can be given in terms of the following mechanism:

$$NO_2^- + C \rightleftharpoons (NO_2)C + e, \quad (Ia)$$

$$(NO_2)C \rightarrow NO_2^+ + C + e, \quad (IIb)$$

$$NO_2^+ + NO_2^- \rightleftharpoons (N_2O_4) \rightleftharpoons 2NO_2. \quad (IIIb)$$

With the same assumptions already mentioned with reaction (IIa) as the rate-determining step, the rate equation coming out from this mechanism of reaction, involving reaction (IIb) as the rate-determining step, is the same as (7). The NO_2^+ ion is proposed here as a short-lived intermediate of the electrode reaction.

Consequently it is not possible to decide if (IIa) or (IIb) is the rate-determining step of the anodic process or if both are acting simultaneously.

Data from decay curves are fairly strongly dependent on the state of the electrode surface. This fact makes any possible evaluation of pseudocapacitance uncertain and may be considered as the cause of a certain non-reproducibility of those curves. Nevertheless, the magnitude of any pseudocapacitance may be low, as far as the foregoing interpretation of steady current/voltage curves is concerned.

Values of t' obtained from the decay curves were rather scattered. The same is true for some slopes obtained from the semilogarithmic plot, especially those recorded at intermediate current densities, which are sometimes lower than $2RT/3F$. The

interpretation of decay curves can be based on various possibilities. Considering that at current interruption the net electrolysis current is nil, although both faradaic and capacitative processes are taking place in the electrical double layer, we can write

$$i_a = \Sigma i_F + \Sigma i_C = 0, \tag{8}$$

where i_F and i_C are respectively the faradaic and capacitative contributions to the current. Equation (8) is related to various types of processes occurring at current interruption.

(i) If the potential decay is due to the rate of dissappearance of reaction intermediates in the electrical double layer, through a reaction such as (IIa), the slope of the linear portion of the $\eta/\log t$ plot must coincide with the slope obtained from the current/voltage curves, as already known.[16]

(ii) A second possibility emerges if during the electrode discharge process the participation of the following reaction takes place:

$$(NO_2)C + (NO_2)C \rightarrow (N_2O_4) + 2C. \tag{IVa}$$

If the discharge mechanism depends on reaction (IVa), mathematical treatment would yield a linear relationship between η and $\log t$ within a certain potential range, with a slope $RT/2F$.

(iii) Another possible path for the disappearance of the intermediate is through the reverse of (Ia). If this reaction is included in the decay mechanism together with (IIa), the number of intermediates disappearing in a certain time should be larger than in case (i). The decay slope would then approach the value $2RT/F$.

Cases (i) and (ii), which involve a constant electrode capacitance during the decay process, may give an explanation of the type of decay curves, as far as their slope in the $\eta/\log t$ plot is concerned, but they fail to show the variation of t' previously mentioned. The latter effect may be considered as follows.

(iv) The potential decay does not conform strictly to case (i) as would occur if the reaction during decay could be assigned to a simple model. The decay slopes and values of t' can hardly be related, at least with the present results, to the existence of an intermediate degree of coverage.[16] According to the likely mechanism of the anodic reaction involving reaction (IIa) as the rate-determining step, the electrode potential is determined by the actual surface activity of the intermediate compound. If it does not disappear at the rate expected for case (i) it is possible that part of the entities participating in the discharge process are replaced by others coming from the inner part of the electrode up to the reaction surface. The latter effect might be related to a diffusion of nitrogen dioxide from the bulk of the electrode outwards to participate either in reaction (IIa) or in reaction (IIb). This new picture of the decay process can be expressed

$$i_F + i_C + i_P = 0, \tag{9}$$

where

$$i_F = i_0 \exp [3F\eta/2RT], \tag{10}$$

$$i_C = C_{DL} \frac{d\eta}{dt}, \tag{11}$$

and i_P is a diffusional current density related to the mass transfer within the porous electrode. A rigorous equation for the latter is unknown but as an approximate solution, taking into account the porosity of the electrode material, the equation of unidirectional planar diffusion can be used.[17] Thus we have

$$i_P = \frac{FD_i^{1/2}C_i}{\pi^{1/2}t^{1/2}}, \tag{12}$$

where C_i is the concentration of the diffusing species in the bulk of the electrode and D_i its diffusion coefficient. From (9)–(12), at $t \to 0$, and anodic potentials sufficiently distant from equilibrium, we get

$$i_0 \exp [3F\eta/2RT] + \frac{FD_i^{1/2}C_i}{\pi^{1/2}t^{1/2}} = -C_{DL}\frac{d\eta}{dt}. \tag{13}$$

At $t \to 0$, if the decay process is diffusion-controlled from the bulk of the electrode, the limiting expression obtained after integration of (13) yields a linear decay of the overvoltage with $t^{1/2}$. Experimental data shown in the decay curves approaches this relationship at $t \to 0$. Another limiting equation results when i_P can be neglected as compared to i_F. In this case the known η/log t relationship results, comprising a decay slope coincident with the Tafel slope from steady current/voltage curves.

The decay curves will be rather more complicated in the intermediate kinetic region than either that expected from the simple discharge of the Helmholtz double layer through a faradaic process or that due to the existence of reaction intermediates at the interphase. They may, therefore, still fit, within a certain potential range,

$$\eta = \text{const} - b_d' \ln (t + t'); \tag{14}$$

but the existence of the diffusional process in the non-steady measurements, even in the case of the simple type of diffusion imagined, yields a dependence of t' on a set of variables related to the diffusion as well as the faradaic process, so that the decay of the anode potential becomes a problem difficult to handle accurately under the present circumstances.

Consequently, case (iv) yields a rather likely qualitative picture of the decay process, which is also supported by the mechanism postulated from steady state measurements.

Besides any other surface-oxidation process, the very complex nature of the electrode material leaves open some uncertainty about the effect of temperature on the anodic process; there is no definite change of the exchange current density with temperature. It is likely that the electrochemical reaction involves a low interaction energy between the products and the electrode surface, and that the electrode surface changes with temperature. If both effects are acting simultaneously and in the opposite way, the apparent effect of temperature on the exchange current density may be within experimental error.

Nevertheless, as the Tafel slope is the same for the whole temperature range investigated, it can be concluded with some certainty that the mechanism of the electrode process is not modified. Finally, the fact that there is no appreciable electrode consumption during the reaction, as in the case of the electrolysis of molten

nitrates on graphite electrodes,[10] supports the previous idea of a small interaction between the intermediate compounds and the graphite lattice. This effect can be attributed to a localization of the reactivity of the intermediate compound on the nitrogen atom, showing a strong tendency to stabilize through the dimer molecule formation, in equilibrium with nitrogen dioxide.

Acknowledgements—This work was supported with funds of the Consejo Nacional de Investigaciones Cientificas y Técnicas of Argentina. The authors are indebted to Prof. P. Rivarola of the University of Cuyo, for the porosity determinations.

REFERENCES

1. A. J. CALANDRA and A. J. ARVÍA, *Electrochim. Acta* **11**, 1173 (1966).
2. A. J. CALANDRA and A. J. ARVÍA, *Electrochim. Acta*, **12**, 95 (1967).
3. YU. S. LYALIKOV, *Zh. analit. Khim.* **8**, 38 (1953); *Chem. Abstr.* **47**, 5273a (1953).
4. YU. S. LYALIKOV and R. M. NOVIK, *Uchen. Zap. kisch. gos. Univ.* **27**, 61 (1957); *Chem. Abstr.* **54**, 22101d (1960).
5. H. S. SWOFFORD, JR. and P. G. MCCORMICK, *Analyt. Chem.* **37**, 970 (1965).
6. G. DELARUE, *J. electroanal. Chem.* **1**, 13, 285 (1959/60);
7. D. INMAN and J. BRAUNSTEIN, *Chem. Commun.* 148 (1966).
8. M. E. MARTINS, A. J. ARVÍA and A. J. CALANDRÁ, in preparation.
9. D. J. E. INGRAM and D. E. G. AUSTEN, in *Industrial Carbon and Graphite*, p. 19. Soc. Chem. Ind., London (1958).
10. A. J. ARVÍA and W. E. TRIACA, *Electrochim. Acta* **11**, 975 (1966).
11. W. E. TRIACA and A. J. ARVÍA, *Electrochim. Acta* **10**, 409 (1965).
12. A. J. ARVÍA, A. J. CALANDRÁ and H. VIDELA, *An. Asoc. quím. Argent.* **54**, 143 (1967).
13. B. E. CONWAY, in *Modern Aspects of Electrochemistry*, No. 3, ed. J. O'M. Bockris and B. E. Conway, Chap. 5. Butterworths, London (1964).
14. A. J. ARVÍA and H. J. VANDENBROELE, *An. Asoc. quím. Argent.*, in press.
15. L. C. de TORRE and A. J. ARVÍA, in preparation.
16. B. E. CONWAY and P. L. BOURGAULT, *Trans. Faraday Soc.* **58**, 593 (1962).
17. P. DELAHAY, *New Instrumental Methods in Electrochemistry*. Interscience, New York (1954).